

Concentration measurements of complex mixtures of broadband absorbers by widely tunable optical parametric oscillator laser spectroscopy

K. Ruxton^{*a}, N.A. Macleod^b, D. Weidmann^b, G.P.A. Malcolm^a and G.T. Maker^a

^aM Squared Lasers Ltd., 1 Kelvin Campus, West of Scotland Science Park, G20 0SP, Glasgow, UK

^bSpace Science & Technology Department, STFC Rutherford Appleton Laboratory, Harwell Oxford Campus, Didcot, Oxfordshire, UK

ABSTRACT

The ability to obtain accurate vapour parameter information from a compound's absorption spectrum is an essential data processing application in order to quantify the presence of an absorber. Concentration measurements can be required for a variety of applications including environmental monitoring, pipeline leak detection, surface contamination and breath analysis. This work demonstrates sensitive concentration measurements of complex mixtures of volatile organic compounds (VOCs) using broadly tunable mid wave infrared (MWIR) laser spectroscopy. Due to the high absorption cross-sections, the MWIR spectral region is ideal to carry out sensitive concentration measurements of VOCs by tunable laser absorption spectroscopy (TLAS) methods. Absorption spectra of mixtures of VOCs were recorded using a MWIR optical parametric oscillator (OPO), with a tuning range covering 2.5 μm to 3.7 μm . The output of the MWIR OPO was coupled to a multi-pass astigmatic Herriott gas cell, maintained at atmospheric pressure that can provide up to 210 m of absorption path length, with the transmission output from the cell being monitored by a detector. The resulting spectra were processed by a concentration retrieval algorithm derived from the optimum estimation method, taking into account both multiple broadband absorbers and interfering molecules that exhibit narrow multi-line absorption features. In order to demonstrate the feasibility of the concentration measurements and assess the capability of the spectral processor, experiments were conducted on calibrated VOCs vapour mixtures flowing through the spectroscopic cell with concentrations ranging from parts per billion (ppb) to parts per million (ppm). This work represents as a first step in an effort to develop and apply a similar concentration fitting algorithm to hyperspectral images in order to provide concentration maps of the spatial distribution of multi-species vapours. The reported functionality of the novel fitting algorithm makes it a valuable addition to the existing data processing tools for parameter information recovery from recorded absorption data.

Keywords: Laser, optical parametric oscillator, IR absorption spectroscopy, mixed vapour, spectral fitting.

1. INTRODUCTION

Tunable laser absorption spectroscopy (TLAS) is becoming a key tool in the detection, classification and identification of chemical species across a wide range of application areas. The increasing demands of industry require the extraction of additional information from an absorption spectrum including quantification of the concentrations of all absorbing species. Extraction of accurate concentration data from spectral traces can be difficult as there are a number of factors (including pressure, temperature and interfering signals) that can influence the retrieved concentration. A common technique is to use curve fitting algorithms which optimise the match between measured data and reference spectra in an iterative process. The complex nature of these algorithms results in long processing times particularly if the measurement spectrum contains multiple species with overlapping absorption features. Depending on the degree of spectral overlap, the resulting spectra may not be a linear superposition of absorption features. This work presents a technique for the successful deconvolution of absorption spectra containing multiple species with overlapping absorption features to obtain individual concentration information.

* keithr@m2lasers.com, tel: +44(0) 141 945 0500

Optical parametric oscillator (OPO) lasers provide tunable radiation in both the short wave (SWIR, 1.5 μm to 1.8 μm) and mid wave infrared (MWIR, 2.5 μm to 3.7 μm) spectral regions. The MWIR range (2700 cm^{-1} to 4000 cm^{-1}) is of high importance as it contains a number of strong fundamental absorptions for many species of interest. In this region the molecular vibrations include stretching modes of carbon – hydrogen (C-H), oxygen – hydrogen (O-H) and nitrogen – hydrogen (N-H) bonds. Although the majority of volatile organic chemicals (VOC's) contain C-H groups, spectral diversity in this region is relatively small leading to overlapping absorption features which provide a challenge to spectral fitting routines. Other spectral regions (for example overtones of the C-H modes in the 1.5 μm to 1.8 μm region) may provide higher diversity and less overlapping spectra but have absorption cross-sections orders of magnitude weaker than the fundamental modes. Therefore, this work has focused solely on fitting MWIR spectral data but the principle is easily transferrable to the SWIR or any other spectral region. The broad tunability of the source allows a large spectral window to be accessed which covers multiple absorption features. Multi-pass absorption cells provide long path lengths (~ 200 m) in a compact bench-top package. Well-defined concentrations of single or multiple species can be supplied using a gas generator based on permeation tube technology.

In the present work, we use a combination of an OPO laser, multi-pass absorption and gas generator to generate absorption spectra of single and multiple species in the MWIR spectral region. Concentration data was retrieved from measured traces using an optimum estimation method (OEM) developed from previous work on atmospheric remote sensing [1]. The OEM algorithm performs a global fit of all relevant parameters and offers extensive diagnostic and analysis tools to evaluate the level of confidence in the retrieved concentrations. This includes a full analysis of error propagation throughout the retrieval, which is dominated in most cases by the contribution from random measurement noise. The following sections give a description of the experimental setup, followed by a selection of results using the OEM for vapour concentration retrieval. Conclusions will be made on the effectiveness of using the OEM technique and how it can be used on a laser system to perform accurate concentration measurements in a number of application areas.

2. EXPERIMENT

Figure 1 shows a schematic and photograph of the experimental system used to obtain absorption spectra. A MWIR pulsed OPO (M Squared Lasers' Firefly-IR) provided radiation in the 2.5 μm to 3.7 μm spectral region. The IR radiation was spatially overlapped with a red visible laser and directed into a multi-pass absorption cell (Aerodyne model AMAC-200) with a nominal path length of 210 m. Small D-shaped mirrors, 0.5 inch diameter, were used to couple the radiation in and out of the cell. The output radiation was focused onto a thermoelectrically-cooled MCT detector, which had an active area of 0.785 mm^2 , using a 3-inch focal length off-axis parabolic mirror. The measured signal as a function of laser wavelength was recorded using software integrated with the laser system. The multi-pass gas cell, which had a volume of 5.1 litres, was connected to the output of the gas-generator by metal tubing. The cell was operated in constant pressure mode at 760 Torr using a pressure controller to simulate a long path at atmospheric pressure.

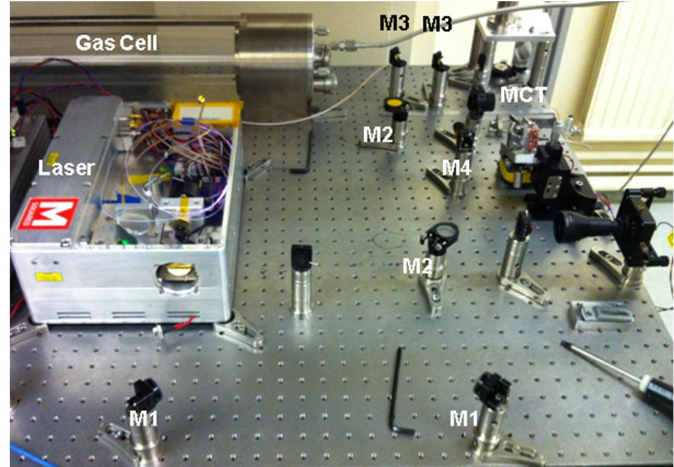
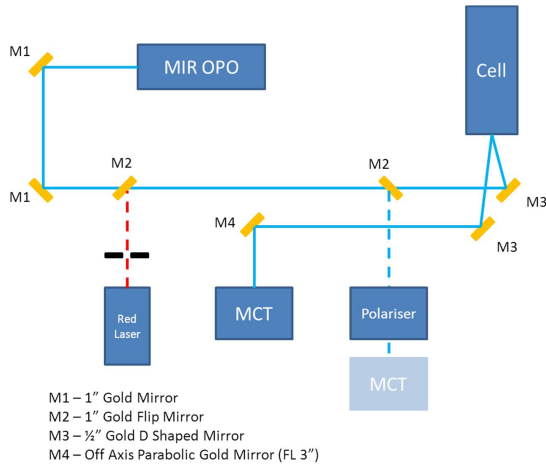


Figure 1. Schematic (left) and photograph (right) of the experimental system used to obtain absorption spectra.

2.1. IR source and detector

The OPO operates inside the resonator of a Neodymium Yttrium Orthovanadate (Nd:YVO₄) laser. This increases the incident power on the OPO compared to an external configuration. The Nd:YVO₄ laser is pumped by an 808 nm laser diode and is Q-switched to increase the peak power of the laser pulses. The pump laser and hence the OPO run at a repetition rate of 150 kHz with a pulse duration of 10 ns. The OPO uses the non-linear optical material Lithium Niobate, which has been periodically poled to allow wavelength selection by simple translation of the crystal in a direction perpendicular to the propagation axis of the laser beam. The OPO generates a pair of wavelengths, called the signal and idler, which are related to the pump wavelength by Equation 1 where λ_{pump} is the wavelength of the Nd:YVO₄ laser (1064 nm) and λ_{signal} and λ_{idler} are the signal and idler wavelengths of the OPO.

$$\frac{1}{\lambda_{\text{pump}}} = \frac{1}{\lambda_{\text{signal}}} + \frac{1}{\lambda_{\text{idler}}} \quad (1)$$

The non-linear crystal is mounted on a motorised translation stage, which allows the wavelength of the OPO to be tuned under computer control. The typical power characteristics of the idler beam as a function of wavelength is shown in Figure 2.

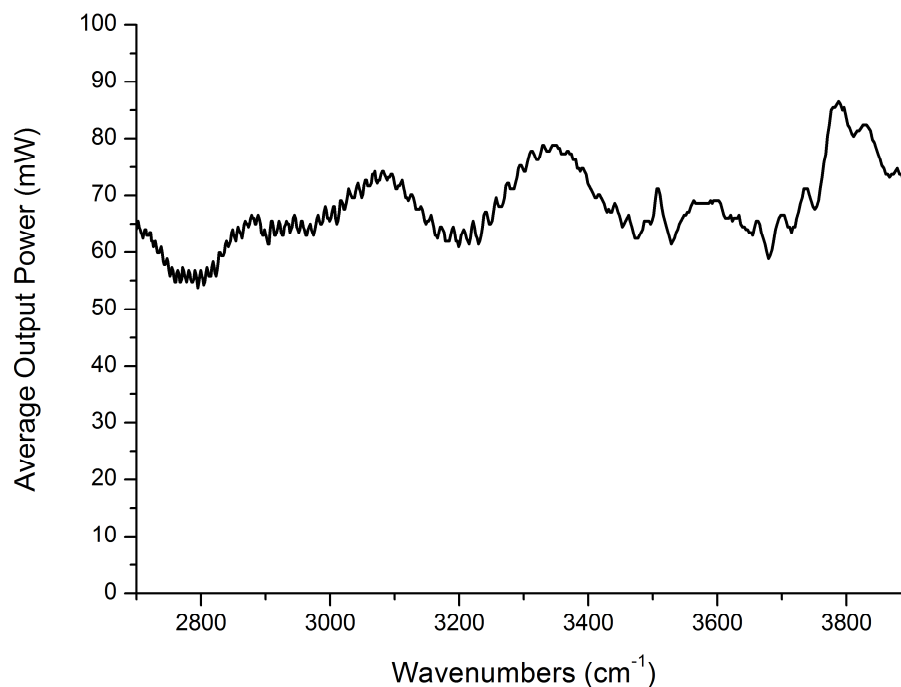


Figure 2. Typical power output of the OPO as a function of wavenumber.

2.2. Gas cell and generator

The actual path length of the multi-pass absorption cell can be estimated by comparison of the spot pattern of the visible alignment laser on the end mirrors with the supplier reference patterns [2]. This appeared to correspond to the maximum possible length of the cell (238 passes at 0.88 m per pass corresponding to a total path length of 209.4 m). Since the path length is a vital input for the multi-species fitting algorithm, the pulsed nature of the OPO laser was exploited to provide an independent check of the path length. The input beam was directed onto the detector using a flip mount. A wire-grid polariser was used to reduce the laser power to avoid damaging the detector. Figure 3 shows a plot of detector signal as a function of time delay for the input and output beams. The time difference between the input and output beams of the multi-pass cell was calculated to be 708.3 ns, giving a total path length difference of 212.5 m. Subtracting the beam path outside the cell, 2.43 m, gave a path length of the cell as 210.07 m. The width of the laser pulse (10 ns) limits the temporal resolution and corresponds to a path difference error of ± 3 m. This measurement of path length agrees well with the value given by the specifications of the cell.

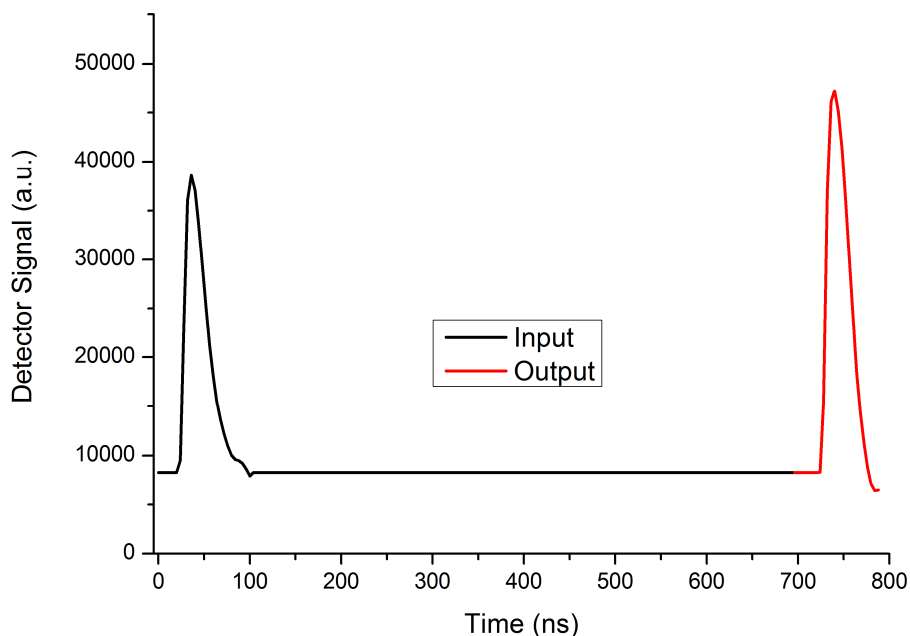


Figure 3. Time dependence of the MCT detector signal for the input (black trace) and output beams (red trace). The power of the input beam was reduced using a wire-grid polarizer to avoid damaging the detector.

The gas cell was supplied by a gas generator, Owlstone OVG-4, which utilised permeation tubes to generate calibrated gas flows. The gas generator had two ovens each with temperature and flow control, which could each hold up to three custom made permeation tubes. The vapour from the tubes were mixed with a nitrogen carrier gas and piped into the cell using 3 m of flexible steel tubing. The concentration of the vapour was calculated from the permeation rate of the compound in the tube and the flow rate of the gas generator. The permeation rate of each tube was measured gravimetrically. By having multiple tubes in the same oven complex mixtures could be generated easily as the compounds mix in their gas phase.

2.3. Calibration – permeation tubes

Permeation tubes containing each of the five VOCs tested were placed in both ovens at a temperature of 50°C. The length of each tube was 5 cm to allow three tubes to be placed in a single oven (total length = 16 cm). The mass of each tube was measured daily over a period of one week to obtain permeation rates. Figure 4 shows mass loss data for each compound as a function of time. Permeation rates, derived from linear fits to the experimental data, are shown in Table 1 along with the calculated concentration at a flow rate of 50 ml/min.

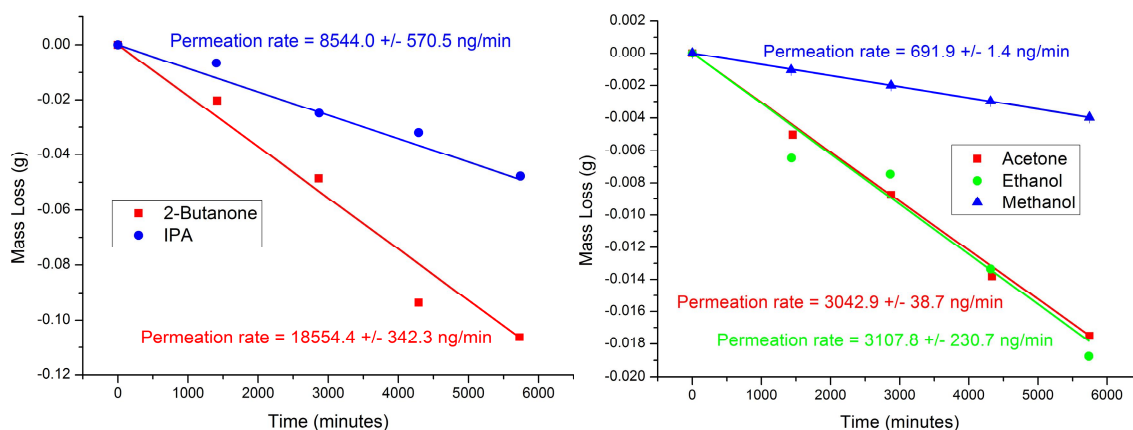


Figure 4. Mass loss data for each of the VOCs at an oven temperature of 50°C. Solid lines are linear fits to the experimental data.

Table 1. Fitted permeation rates and concentrations for the VOCs tested. The concentrations were calculated at a flow rate of 50 ± 0.5 ml/min, a temperature of $21 \pm 1^\circ\text{C}$ and a pressure of 760 ± 5 Torr.

VOC	Permeation rate (ng/minute)	Concentration at 50 ml/minute (ppm)
Acetone	3042.9 ± 38.7	25.3 ± 0.8
2-Butanone (Methyl ethyl ketone)	18554.4 ± 342.3	124.2 ± 4.8
Ethanol	3107.8 ± 230.7	32.6 ± 3.1
IPA	8544.0 ± 570.5	68.6 ± 6.0
Methanol	691.9 ± 1.4	10.4 ± 0.2

2.4. Spectral fitting algorithm

The retrieval of vapour concentration information was performed using the optimum estimation method (OEM) originally developed for atmospheric sounding [3]. The parameters to fit were the concentration of each VOC concatenated into a state vector \vec{x} of dimension n , corresponding to the number of molecular concentrations to retrieve plus baseline, linewidth, of frequency shift parameters if needed. The experimental spectral data provides the measurement vector \vec{y} , of dimension m . The first step consists of building the forward model, which contains all the physics known about the problem, which aims to reproduce as accurately as possible the output data of the instrument. The forward model relates the state vector \vec{x} , to the measurement vector \vec{y} , according to Equation 2:

$$\vec{y} = F(\vec{x}) + \vec{\varepsilon} \quad (2)$$

where the function F represents the forward model, and $\vec{\varepsilon}$ is the error vector accounting for the mismatch between the model's results and the measurements. The retrieval problem consists of inverting equation 2 and solving for \vec{x} , knowing \vec{y} .

To constrain the inverse problem further, a set of a-priori data on the fitted parameters is necessary. These will include all the known a-priori knowledge on the parameters being retrieved. The a-priori data forms the a-priori vector \vec{x}_a , while the uncertainties on the a-priori data are incorporated into the a-priori covariance matrix S_a . In addition, the imperfection of the measurements is accounted for via the measurement covariance matrix S_E .

If we assume that the measurement complexity is such as the central limit theorem applies, the error statistics will be Gaussian and the problem will follow theorems of Bayesian information. Inverting the problem becomes the minimisation of a cost function χ^2 defined by Equation 3:

$$\chi^2 = [\vec{y} - F(\vec{x}_n)] \cdot S_E^{-1} \cdot [\vec{y} - F(\vec{x}_n)]^T + [\vec{x}_a - \vec{x}_n] \cdot S_a^{-1} \cdot [\vec{x}_a - \vec{x}_n]^T \quad (3)$$

With χ^2 minimized, \vec{x}_n is the best estimator of \vec{x} . For a moderately non-linear inversion problem, a local linearisation of equation 2 becomes:

$$\vec{y} = K \cdot \vec{x} + \vec{\varepsilon} \quad (4)$$

where K is the Jacobian matrix or the set of weighting functions. The components of the K matrix inform us on the sensitivity of the forward model to the concentrations. The iterative Levenberg-Marquardt approach is used to converge

towards the best estimate of \vec{x}_n by minimising χ^2 according to the following algorithm relating the state vector for the iteration $i+1$ to the one from the iteration i :

$$\vec{x}_{i+1} = \vec{x}_i + [(1 - \lambda)S_a^{-1} + K_i^T \cdot S_\epsilon^{-1} \cdot K_i]^{-1} \cdot [K_i^T \cdot S_\epsilon^{-1} \cdot (\vec{y}_1 - F(\vec{x}_i)) + S_a^{-1} \cdot (\vec{x}_a - \vec{x}_i)] \quad (5)$$

where λ is the Levenberg-Marquardt dampening parameter which is set to offer a good trade off between convergence speed and accuracy of the estimation. The forward model includes line by line calculation of transmission spectra based on the HITRAN database [4] for atmospheric species if required. For broadband absorbers such as the VOC's measured in this work, absorption cross-section reference data from the PNNL database is used as input data [5]. After the transmission is calculated, convolution with a Gaussian lineshape (FWHM = 5 cm⁻¹) accounts for the laser linewidth contribution to the spectrum.

3. RESULTS

Experimental spectra were obtained by monitoring the detector signal of the output of the cell as a function of laser wavelength. A background scan of the cell was obtained with a pure flow of nitrogen gas from the gas generator with no permeation sources loaded in the ovens. Spectra of the individual VOC's (except for 2-butanone) were obtained at the maximum concentration possible using the slowest possible flow rate (50 ml/min). The spectrum of acetone was obtained using a single oven while that of isopropyl alcohol (IPA) was measured using a configuration with the output of both ovens attached to the cell. The output of a single oven was used to provide a mixture of 3 species, acetone, methanol and ethanol, while both ovens were linked together to give a mixture of 5 species, the above three species plus IPA and 2-butanone (methyl ethyl ketone).

3.1. One species mixture

Figures 5 and 6 show the results of the forward model fitting of the experimental data obtained with a single species (acetone or IPA) in the cell. The fitted concentrations from the spectral fitting routine, given in Table 2, are about 3.7 times smaller than the nominal acetone concentration delivered by the generator and 10.8 times smaller in the case of IPA. This drop is due to the 3 m of metal tubing connecting the output of the gas generator to the input of the gas cell.

The acetone fit matches the experimental trace to within $\pm 2\%$ at worst, with the exception of issues in reproducing the sharp feature at ~ 2980 cm⁻¹. This is clearly observed in the residuals between the measured and fitted traces and indicates an imperfect modelling of the laser linewidth. The laser linewidth of the OPO system is known to vary during the wavelength scan, whereas the model incorporates a fixed Gaussian laser linewidth. In addition, the laser noise increases at higher wavenumber (this has been observed in all measurements), and at frequencies greater than 3500 cm⁻¹ oscillations in the signal are observed. This excess noise, along with large residual oscillations indicates a background correction issue. The IPA fit matches the experimental trace within $\pm 5\%$ and indicates similar mismatching as found in the acetone case.

The right hand plots of Figures 5 and 6 show the averaging kernels (AK) from the OEM fit. For high quality retrieval, the AK of each retrieved parameter should peak at a value of one for the corresponding parameter, and remain zero for the other. The AK matrix for an ideal retrieval should be an identity matrix. If the AK's do not fulfil this requirement, this indicates either information cross-talk between parameters or a lack of sensitivity in the retrieval to the actual values being retrieved. The AK's for the IPA case are a good example of a near ideal situation while those of acetone show a slight negative sensitivity of the wavenumber shift parameter on the acetone concentration.

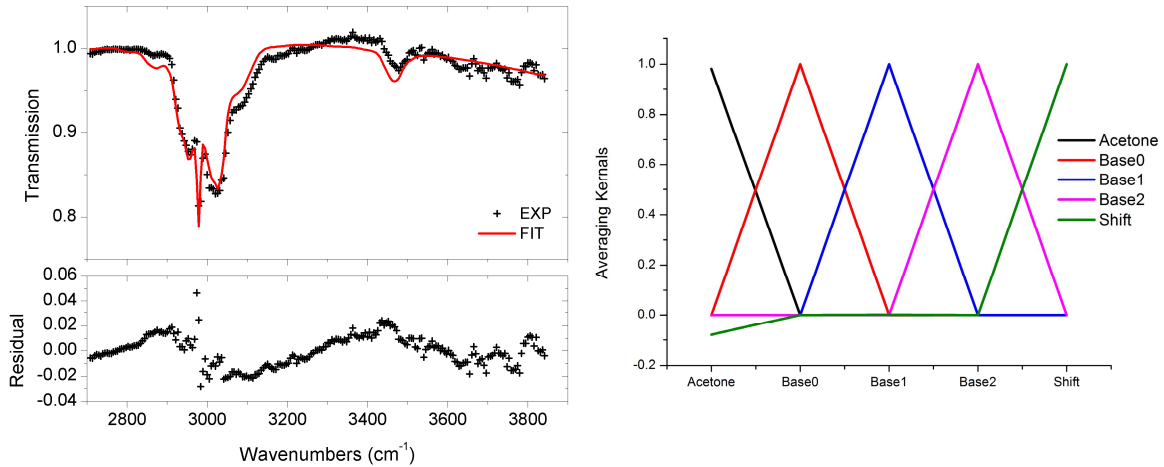


Figure 5. Left, absorption spectra and OEM fit of acetone absorption spectrum. The upper panel shows the measured transmission spectra (black trace) and the OEM fit (red trace) while the lower panel shows the residual between the measured and fitted traces. Right, averaging kernels from the OEM fit for the 5 fitted parameters.

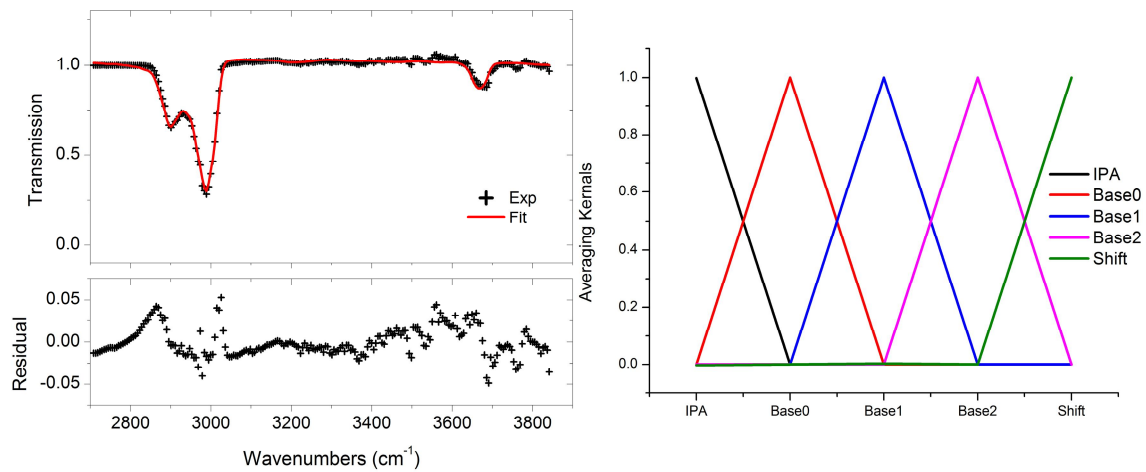


Figure 6. Left, absorption spectra and OEM fit of IPA absorption spectrum. The upper panel shows the measured transmission spectra (black trace) and the OEM fit (red trace) while the lower panel shows the residual between the measured and fitted traces. Right, averaging kernels from the OEM fit for the 5 fitted parameters.

Table 2. Fitted parameters from the retrieval algorithm. Parameters retrieved were the vapour concentration of acetone or IPA, three quadratic baseline coefficients to correct for discrepancies in the background correction, and a wavenumber shift parameter to account for any mismatch in the frequency calibration.

Species	Concentration (ppm)	Base0	Base1	Base2	Shift (cm ⁻¹)
Acetone	6.54 ± 0.08	1.002 ± 0.002	(2.1 ± 0.3)10 ⁻⁴	(-1.64 ± 0.13)10 ⁻⁶	-8.21 ± 0.13
IPA	6.36 ± 0.03	1.030 ± 0.002	(1.8 ± 0.3)10 ⁻⁴	(-1.20 ± 0.14)10 ⁻⁶	-10.38 ± 0.11

3.2. Three species mixture

As a further test of the capabilities of the OEM fitting routine a series of multi species vapours were produced by the gas generator and interrogated by the IR source. Figure 7 shows the results for a 3 species mixture consisting of ethanol, methanol and acetone. One of the first observations is that the distinct triple peak absorption feature of acetone is washed out in the mixture spectrum in the C-H stretching (3000 cm^{-1}) region, due to overlapping absorption features from the other two species. Outputs from the retrieval algorithm are given in Table 3. As was found for single species measurements, the concentrations measured are much lower than generated due to the long transfer line between the gas generator and the cell. It is interesting to note that the acetone concentration is reduced in the mixture in comparison to the previous case of a single acetone permeation source in the oven.

The fit to the experimental data matches within $\pm 10\%$. The main source of error is due to the model itself, which in this case is much larger than the measurement error, and is perceptible through a combination of lineshape mismatch and imperfect frequency calibration. The AK's shown in the right hand side of Figure 7, indicates that information obtained on methanol and ethanol is fully reliable, whereas in the case of acetone only a part of the information ($\sim 60\%$) is related to the actual acetone concentration with the remaining information originating from the a priori information.

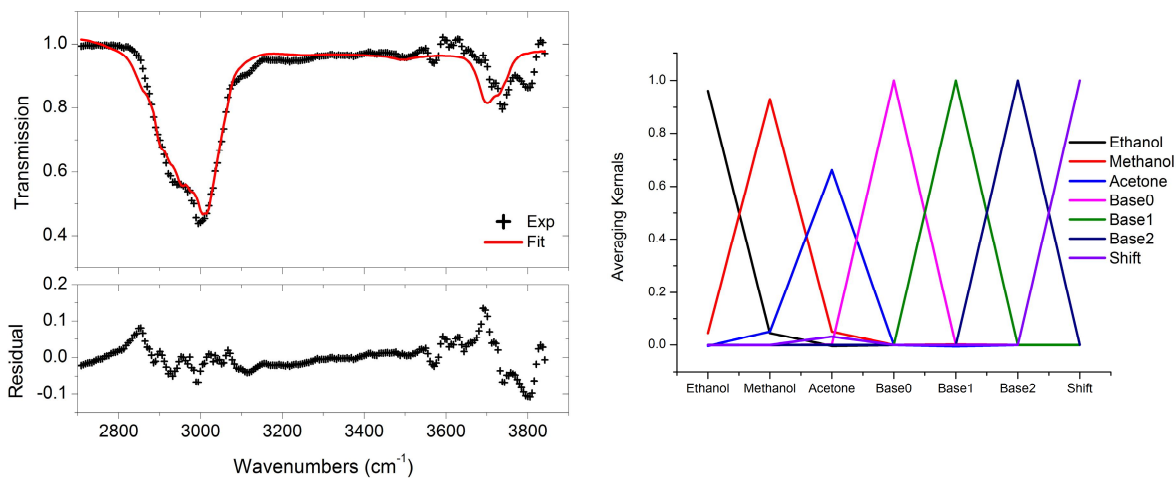


Figure 7. Left, absorption spectra and OEM fit of absorption spectrum for a 3 species mixture containing ethanol, methanol and acetone. The upper panel shows the measured transmission spectra (black trace) and the OEM fit (red trace) while the lower panel shows the residual between the measured and fitted traces. Right, averaging kernels from the OEM fit for the 7 fitted parameters.

Table 3. Fitted parameters from the retrieval algorithm. Parameters retrieved were the vapour concentration of ethanol, methanol and acetone, three quadratic baseline coefficients to correct for discrepancies in the background correction, and a wavenumber shift parameter to account for any mismatch in the frequency calibration.

Acetone (ppm)	Methanol (ppm)	Ethanol (ppm)	Base0	Base1	Base2	Shift (cm^{-1})
4.36 ± 0.09	4.16 ± 0.11	2.10 ± 0.13	1.031 ± 0.002	$(-8.5 \pm 0.3)10^{-4}$	$(2.92 \pm 0.14)10^{-6}$	-33.80 ± 0.03

3.3. Five species mixture

Figure 8 shows results for a 5 species mixture consisting of acetone, ethanol, IPA, methyl ethyl ketone and methanol. The retrieval indicates a match within $\pm 5\%$. The spectrum is dominated by IPA, which combines a high relative concentration with strong absorption cross-sections. Table 4 gives the output parameters returned by the fitting algorithm. The right hand side of Figure 8 shows the AK's as an estimate of the level of confidence in the returned parameters.

In this case, the AKs indicate some clear cross talk. For acetone the sensitivity is rather low, indicated by an AK peaking at 20%. This is further confirmed by examination of the weighting functions shown in the left hand side of Figure 9, where the acetone contribution is clearly the lowest of the five species. The acetone AK also indicates some cross talk

with MEK. Only about 40% of information related to the actual concentration of ethanol is retrieved by the fit and a similar value is found for methanol. These two molecules also display significant cross talk. MEK exhibits an almost full sensitivity (80%) while IPA is the dominant signal which is retrieved with the highest level of confidence. The AK related to the wavenumber shift shows that through a better spectral absolute spectral calibration, improvements in the retrieved parameters should be possible via minimization of the information leakage from the shift to the molecular concentrations.

To investigate further the retrieval behaviour, the gain matrix G can be examined. This provides the sensitivity of the retrieved parameters (VOCs' concentration) to the measurement vector (transmission spectrum). In other words, the spectral zones giving the most information on the molecular concentration can be analysed. The normalized absolute values of the gain functions are shown in the right hand side of Figure 9, with the focus placed on the spectral areas with significant gain, i.e. those where absorption features exist. The plot shows that in principle, except for IPA, there are different spectral areas with non overlapping gain for the four other VOCs. However, the absolute gain scales with the strength of the absorption signal, therefore to obtain good sensitivity to all VOCs in a mixture either no individual VOC should dominate the transmission signal, or the measurement noise needs to be very low to capture tiny amount of spectral signal variation.

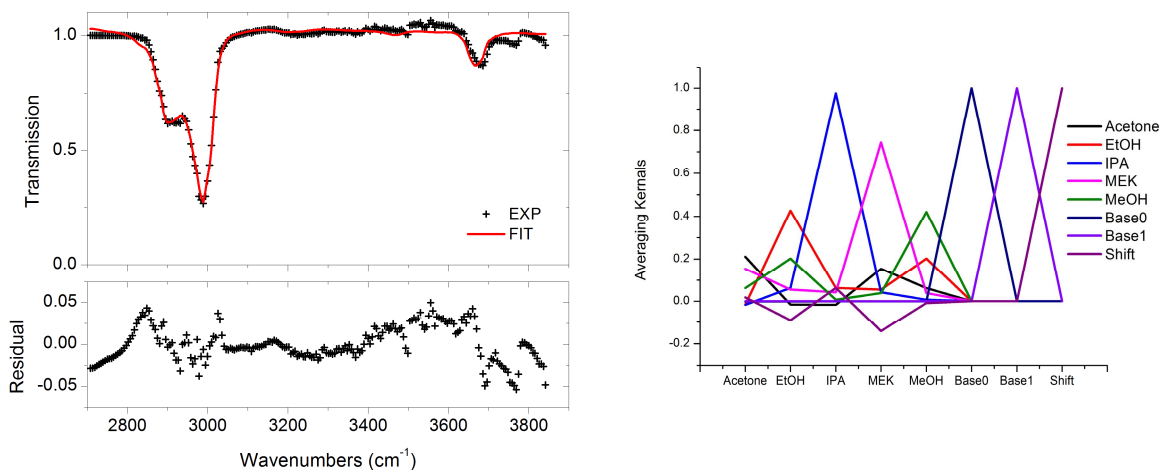


Figure 8. Left, absorption spectra and OEM fit of absorption spectrum for a 5 species mixture containing acetone, ethanol, IPA, methyl ethyl ketone and methanol. The upper panel shows the measured transmission spectra (black trace) and the OEM fit (red trace) while the lower panel shows the residual between the measured and fitted traces. Right, averaging kernels from the OEM fit for the 8 fitted parameters.

Table 4. Fitted parameters from the retrieval algorithm. Parameters retrieved were the vapour concentration of acetone, ethanol, IPA, methyl ethyl ketone and methanol, linear baseline coefficients to correct for discrepancies in the background correction, and a wavenumber shift parameter to account for any mismatch in the frequency calibration.

Acetone (ppm)	EtOH (ppm)	IPA (ppm)	MEK (ppm)	MeOH (ppm)	Base0	Base1	shift
0.78 ± 0.07	0.95 ± 0.08	4.93 ± 0.08	1.74 ± 0.09	0.68 ± 0.06	$1.048 \pm .001$	$(14.9 \pm 0.87)10^{-5}$	-9.2 ± 0.09

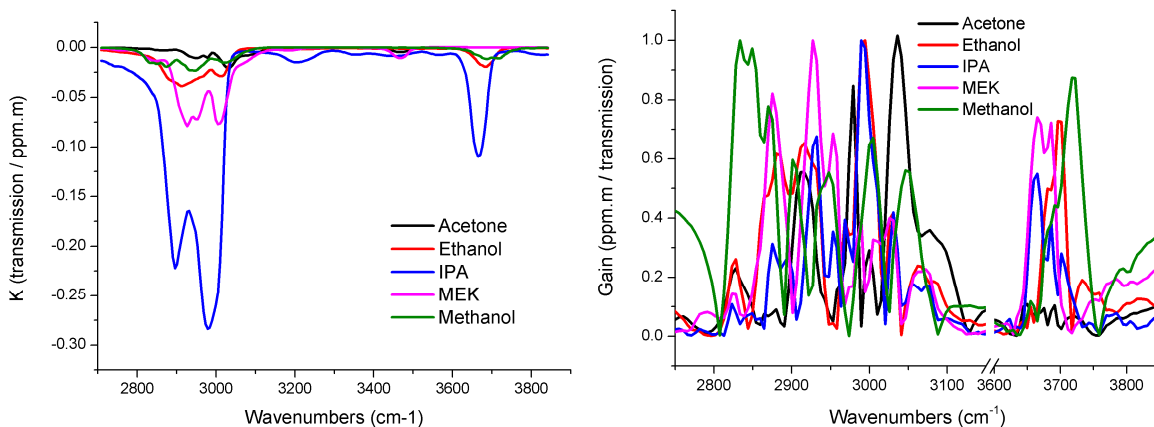


Figure 9. Further analysis of the five VOCs fit showing the weighting functions (left) and the normalized absolute value of the gain functions (right)

4. CONCLUSION

This feasibility work has shown the successful retrieval of vapour concentration information from experimental absorption spectra in the mid-infrared spectral region using the OEM approach. The algorithm has been applied to both single and multi-species absorption. Laser radiation is provided by an OPO laser system. The broad tunability available covers multiple absorption features using a single source, which aids the retrieval process by covering a large spectral window. For this work the concentration drop induced by long delivery tubing has introduced mismatch between the calibrated concentration and the one measured inside the multi-pass cell. Work is underway to integrate the retrieval algorithm directly into a post-processing FPGA as an integral part of the laser system to perform near real time measurements of concentrations. The work has indicated a number of developments for the laser system, which will lead to increased performance of the retrieval. Improvements will be seen from pulse to pulse normalisation of the input and output pulses giving baseline free traces less prone to pulse to pulse variation. This will eliminate baseline parameters and will reduce the measurement noise and yield greater concentration sensitivity. The retrieval analysis has also identified that improved laser calibration of wavelength and linewidth should reduce the cross talk between retrieved concentrations and ensure that the forward model matches the measured signal with a higher level of accuracy. The exact laser linewidth shape should also be measured to improve the forward model accuracy.

Following this feasibility demonstration, further experimental work will be undertaken with a larger level of control on mixture concentration (reduced adsorption) with the improvements previously described implemented. Then, extension of the retrieval algorithm to multi-pixel detection will be undertaken for complex mixture concentration imaging.

ACKNOWLEDGEMENTS

The financial support of Scottish Enterprise as part of the Explosive Detection Platform project is acknowledged.

REFERENCES

- [1] Weidmann, D., Reburn, W.J. and Smith, K.M., "Retrieval of atmospheric ozone profiles from an infrared quantum cascade laser heterodyne radiometer: results and analysis," *Applied Optics* 46(29), 7162-7171 (2007).
- [2] McManus, J.B., Kebabian, P.L. and Zahniser M.S., "Astigmatic mirror multipass absorption cells for long-path length spectroscopy," *Applied Optics* 34(18), 3336-3348 (1995).
- [3] Rodgers, C.D., [Series on atmospheric, oceanic and planetary physics-Volume 2, Inverse methods for atmospheric sounding, theory and practice], World Scientific Publishers, Singapore, (2000).

[4] Rothman, L.S etal, "The HITRAN 2008 molecular spectroscopic database," Journal of Quantitative Spectroscopy and Radiative Transfer 110, 533-572 (2009).

[5] Sharpe, S,W., Johnson, T.J., Sams, R.L., Chu, P.M., Rhoderick and Johnson, P.A., "Gas-phase databases for quantitative infrared spectroscopy," Applied Spectroscopy 58(12), 1452-1461 (2004).